Evaluation of Dynamic Polar Molecular Surface Area as Predictor of Drug Absorption: Comparison with Other Computational and Experimental Predictors

Katrin Palm, Kristina Luthman,*,† Anna-Lena Ungell,‡ Gert Strandlund,§ Farideh Beigi,|| Per Lundahl,|| and Per Artursson

Department of Pharmacy (Box 580), Department of Organic Pharmaceutical Chemistry (Box 574), and Department of Biochemistry (Box 576), Uppsala University, BMC, SE-751 23 Uppsala, Sweden, and Pharmacokinetics and Drug Metabolism and Medicinal Chemistry, Astra Hässle AB, SE-431 83 Mölndal, Sweden

Received May 18, 1998

The relationship between various molecular descriptors and transport of drugs across the intestinal epithelium was evaluated. The monolayer permeability (P_c) of human intestinal Caco-2 cells to a series of nine β-receptor-blocking agents was investigated in vitro. The dynamic polar molecular surface area (PSA_d) of the compounds was calculated from all low-energy conformations identified in molecular mechanics calculations in vacuum and in simulated chloroform and water environments. For most of the investigated drugs, the effects of the different environments on PSA_d were small. The exception was H 216/44, which is a large flexible compound containing several functional groups capable of hydrogen bonding ($PSA_{d,chloroform} = 70.8$ Å^2 and $PSA_{d,water} = 116.6$ Å^2). The relationship between P_c and PSA_d was stronger than those between P_c and the calculated octanol/water distribution coefficients (log D_{calc}) or the experimentally determined immobilized liposome chromatography (ILC) retention. P_c values for two new practolol analogues and H 216/44 were predicted from the structure−permeability relationships of a subset of the nine compounds and compared with experimental values. The P_c values of the two practolol analogues were predicted well from both PSA_d calculations and ILC retention studies. The P_c value of H 216/44 was reasonably well-predicted only from the PSA_d of conformations preferred in vacuum and in water. The other descriptors overestimated the P_c of H 216/44 100−500-fold.

Introduction

The use of combinatorial chemistry and high throughput screening in the field of drug discovery has increased the demand for biopharmaceutical screening methods, e.g., for prediction of oral absorption. Caco-2 cell monolayers have been successfully used to model passive drug absorption,[1,2] but the model has not yet been fully adapted for screening purposes. The octanol/buffer distribution coefficient (log *D*) therefore remains a common tool for estimating the extent of drug permeation across epithelia, but with varying results.[1,3−5] Some of the shortcomings of using log *D* in modeling epithelial permeability have been attributed to the ability of the solute to form intermolecular hydrogen bonds in both water and octanol.[6] Therefore, the hydrogen-bonding capacity of the molecule has been introduced as an alternative predictor of passive drug absorption.[4,7,8] In addition to the relatively weak relationship between epithelial permeability and log *D*, the traditional methods of measuring log *D* are time-consuming and require relatively large amounts of the substance under investigation.

More efficient drug permeability screening methods are needed; these should be either less time-consuming experimental methods or based on calculated molecular properties. Chromatographic methods are attractive for screening purposes, since they require only small amounts of solute, and it is also possible to automate the process. The use of stationary phases that mimic the lipid bilayer of cell membranes is expected to result in stronger relationships with epithelial permeability than seen when conventional octadecylsilyl silica (ODS) columns are used. One approach is to use stationary phases consisting of covalently bound phosphatidyl moieties (immobilized artificial membranes, IAM).[9,10] Alternatively, immobilized liposome chromatography (ILC), which also incorporates the bilayer structure of the cell membranes, may offer some advantages.[11]

Computational methods used to calculate various physicochemical properties, such as log *D*, often account for the three-dimensional shape of the molecule inadequately. Steric or conformational effects resulting from the formation of intramolecular hydrogen bonds are not taken fully into consideration with these methods. The calculated molecular surface properties of a drug have been shown to be related to many physicochemical properties believed to be relevant to epithelial permeability[12−15] and uptake across the blood−brain barrier.[16] Interestingly, such calculations could be extended to include also the shape and flexibility of the molecule.[17]

In a previous study, we investigated the relationship between molecular surface properties and epithelial permeability for a series of six β-receptor-blocking

* To whom correspondence should be addressed. Present address: Institute of Pharmacy, University of Tromsø, N-9037 Tromsø, Norway.
† Department of Organic Pharmaceutical Chemistry.
‡ Pharmacokinetics and Drug Metabolism.
§ Medicinal Chemistry.
|| Department of Biochemistry.

10.1021/jm980313t CCC: $15.00
Published on Web 12/05/1998

agents.[18] These compounds were selected as model compounds since their absorption after oral administration in humans and their lipophilicity displayed a wide variability. Further, they have similar molecular weights and pK_a values, which minimized the influence of these parameters on the results. The surface properties were found to vary with the molecular conformation. Therefore, to account for the flexibility of the molecules, dynamic averages of molecular surface properties were calculated from all low-energy conformations identified in conformational analyses. We found promising inverse linear relationships between the polar part of the dynamic molecular surface area (PSA_d) and the intestinal epithelial permeability to the drugs in two in vitro models. These relationships were stronger than those between calculated log *D* values (log D_{calc}) and permeability.

Further studies, on 20 structurally diverse but conformationally rigid compounds, suggested that intestinal drug absorption in humans after oral administration could be predicted from PSA_d.[19] PSA_d was also shown to be related to the hydrogen-bonding capacity of the compounds. Other theoretical approaches have been used to explore models based on a large number of calculated structural properties using PLS methodology[20,21] or considerably simpler but still powerful classification systems.[22] In these studies the hydrogen-bonding/polar component has generally been the dominating factor in predicting epithelial permeability to drugs.

In this paper we extend our evaluation of PSA_d as a predictor of passive epithelial permeability. The first objective was to investigate whether the use of simulated solvent environments instead of vacuum in the Monte Carlo-based conformational searches would influence the calculated dynamic surface properties of nine model drugs and subsequently improve the correlations with epithelial permeability. The molecular mechanics calculations were therefore performed in simulated chloroform or water environments and compared to the results from calculations in vacuum.

The second objective was to compare more closely the two computational predictors PSA_d and log D_{calc}. The descriptors were used in predictions of the permeability of Caco-2 cell monolayers (P_c) to two synthesized analogues of practolol (H 95/71 and H 244/45) from the structure−permeability relationships of the previously studied model drugs (in ref 18). H 95/71 and H 244/45 were designed to display similar polar surface area to that of practolol but to differ in their distribution in octanol/water. The predicted permeabilities were then compared with experimental results. In addition, a structurally different β-receptor antagonist (H 216/44) previously shown to be an outlier in the relationship between log *D* and cell monolayer permeability[23] was investigated.

The third objective was to compare the computational PSA_d method with a new experimental chromatographic screening method, using immobilized liposome chromatography.[11] In ILC, the stationary phase consists of liposomes immobilized in porous gel beads. Retention of solute on these columns is assumed to reflect an interaction of the solute with a lipid bilayer.

Scheme 1. Synthesis of H 95/71 and H 244/45[a]

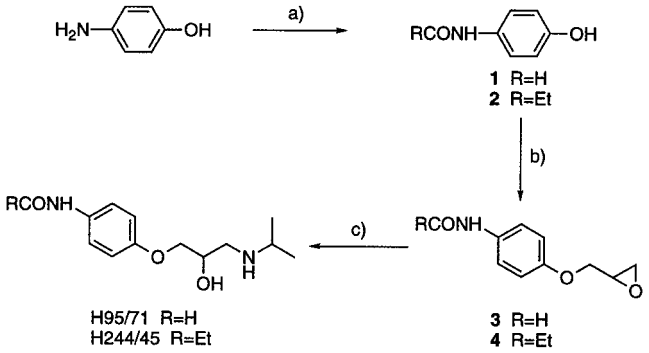

[a] (a) Propionic anhydride or formic acid; (b) epichlorohydrin, KOH; (c) 2-propylamine.

Results and Discussion

Chemistry. Two practolol analogues, H 95/71 and H 244/45, were synthesized using the synthetic pathway described in Scheme 1. Treatment of 4-aminophenol with formic acid or propionic anhydride afforded the acylated derivatives **1** and **2**, respectively. Alkylation of **1** or **2** using epichlorohydrin in the presence of base followed by an epoxide ring opening using isopropylamine produced the target compounds.

Effects of Different Solvation Models Used in Conformational Analyses. A. Conformational Preferences. A large number of low-energy conformations ($\Delta E_s \leq 2.5$ kcal/mol) were identified for all compounds except H 216/44 in the Monte Carlo conformational searches. In general, slightly fewer conformers were identified in the simulated chloroform environment compared to vacuum, and most compounds proved to be most flexible in simulated water. (For detailed information about the number of low-energy conformations identified in each environment, see the Supporting Information.) Surprisingly, only one low-energy conformation resulted from an extensive conformational search of H 216/44 in the water environment (see Experimental Section), while 36 and 6 conformations were found within 2.5 kcal/mol of the global minimum in the vacuum and chloroform environments, respectively. H 216/44 has many rotatable bonds, and the use of continuous solvent simulations dramatically increased the amount of CPU time needed to obtain reliable conformational information. However, all conformations obtained from the vacuum and chloroform Monte Carlo searches which were within the search window (7 kcal/mol) were energy-minimized in the water environment to further validate the result. None of these conformations were found to be within 2.5 kcal/mol of the global minimum conformation identified in the Monte Carlo searches of H 216/44 in simulated water.

The conformational preferences of atenolol, practolol, pindolol, metoprolol, oxprenolol, and alprenolol identified by the Monte Carlo search in vacuum corresponded well with those obtained previously by a stepwise conformational search strategy.[18] The conformational preferences of the 2-hydroxy-3-(isopropylamino)propoxy substituent of H 95/71 and H 244/45 were similar to those of practolol. Many conformations were stabilized by intramolecular hydrogen bonds between both the amine and alcohol, and the alcohol and ether function-

Table 1. Structure of the β-Adrenoreceptor-Blocking Agents

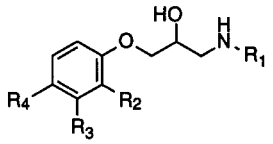

Compound	R_1	R_2	R_3	R_4	pK_a	MW
A. H 216/44	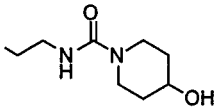	H	H	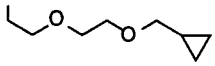	8.5[a]	479
B. atenolol	$CH(CH_3)_2$	H	H		9.6[a]	266
C. H 95/71	$CH(CH_3)_2$	H	H		9.5	252
D. practolol	$CH(CH_3)_2$	H	H		9.5[a]	266
E. H 244/45	$CH(CH_3)_2$	H	H	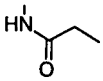	9.5	280
F. pindolol	$CH(CH_3)_2$			H	9.7[a]	248
G. metoprolol	$CH(CH_3)_2$	H	H		9.7[a]	267
H. oxprenolol	$CH(CH_3)_2$	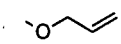	H	H	9.5[a]	265
I. alprenolol	$CH(CH_3)_2$		H	H	9.6[a]	249

[a] From ref 46.

alities. However, amide bond conformations differed; in H 95/71 a *cis*-amide conformation was preferred, whereas *trans*-conformations were favored in practolol and H 244/45.[24]

Only small differences in the conformational preferences of compounds **B**−**I** (Table 1) could be observed between results from conformational analyses performed in vacuum and those performed in simulated chloroform. However, low-energy conformations identified in simulated water showed marked differences in the intramolecular hydrogen-bonding pattern from those seen in the other solvation models. Fewer intramolecular hydrogen bonds were observed in water, indicating an increased interaction of polar groups with the solvent. Interestingly, a preference for conformations stabilized by aliphatic−aromatic interactions was also noted in water. The conformational preferences of H 216/44 clearly differed between vacuum and the two solvents. With this molecule, folded conformations stabilized by intramolecular hydrogen bonds were identified in vacuum and chloroform, whereas more stretched conformations were preferred in water (Figure 1).[25]

B. Dynamic Surface Properties. The low-energy conformations identified for each compound varied in their surface properties (see Figures 2 and 3 and Supporting Information). The variations in polar surface area (differences between the largest and smallest PSA calculated for each compound) ranged from 11 to 47 Å^2 and corresponded to 6−54% of the dynamic averages (Table 2).[26] This was not a random variability caused by poor precision in the surface area calculations but was directly attributable to the influence of conformation.[27] The dynamic averages of the polar surface area resulting from conformational analyses in vacuum ($PSA_{d,vacuum}$), simulated chloroform ($PSA_{d,chloroform}$), and simulated water ($PSA_{d,water}$) environments are presented in Table 2.[28] In general, the PSA_d increased in the order vacuum < chloroform < water as a result of changes in intramolecular hydrogen-bonding patterns. Although clear differences were observed in conformational preferences using different simulated solvent environments, the effect on the dynamic average of the molecular surface properties was relatively small for all compounds but H 216/44 (Table 2). The dynamic polar

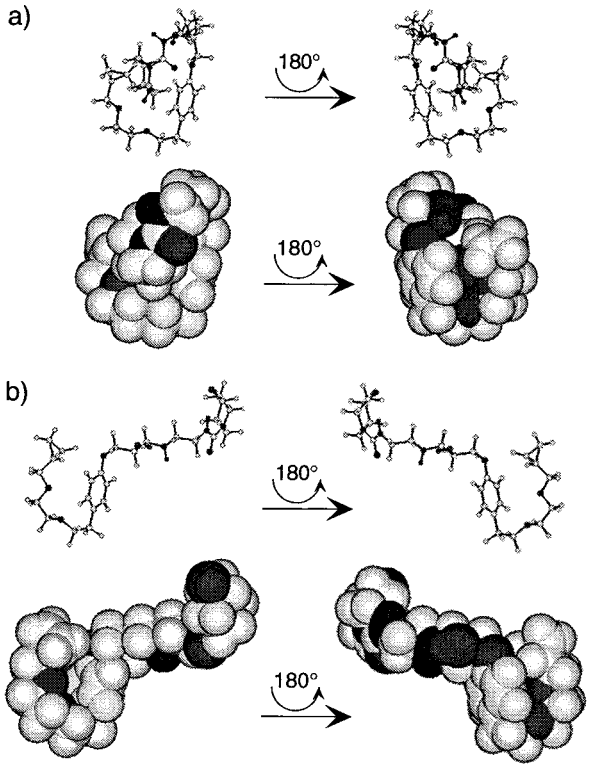

Figure 1. Global minimum conformations of H 216/44 found in Monte Carlo-based conformational searches in (a) vacuum and (b) simulated water environments. Polar areas are displayed in darker colors.

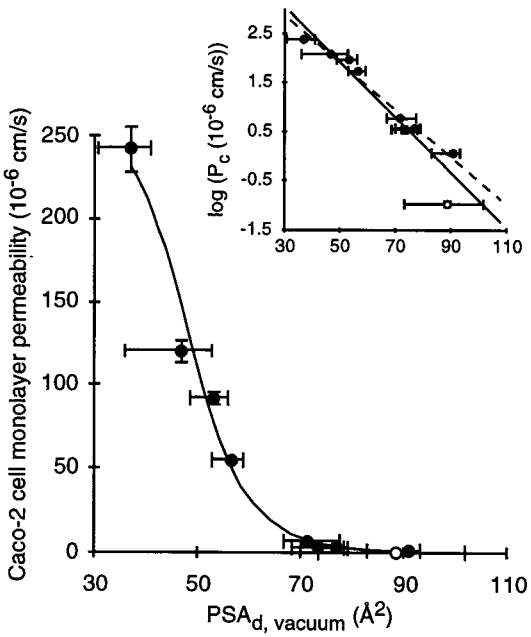

Figure 2. Relationship between $PSA_{d,vacuum}$ of the nine compounds and their Caco-2 cell monolayer permeability coefficients. The insert shows the correlation between log P_c and $PSA_{d,vacuum}$. The dashed line shows the resulting linear correlation when H 216/44 (open circle) is excluded from the data set. Error bars represent SD of P_c and range in $PSA_{d,vacuum}$.

surface area of H 216/44 varied extensively with the solvation model used: 88.7, 70.8, and 116.6 Å^2 in the vacuum, chloroform, and water environments, respectively. These results reflected the larger size and flexibility of H 216/44. The molecule contains many functional groups participating in inter- and intramolecular hydrogen bonds, and the PSA of H 216/44 is therefore sensitive to conformational influences (Figure 1).

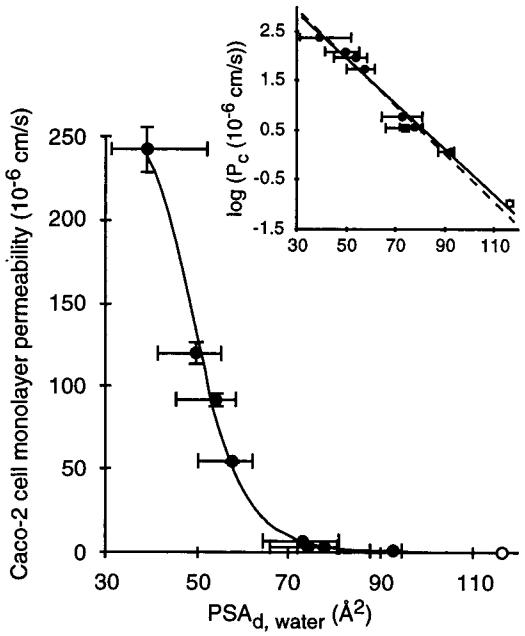

Figure 3. Relationship between $PSA_{d,water}$ of the nine compounds and their Caco-2 cell monolayer permeability coefficients. The insert shows the correlation between log P_c and $PSA_{d,water}$. The dashed line shows the resulting linear correlation when H 216/44 (open circle) is excluded from the data set. Error bars represent SD of P_c and range in $PSA_{d,water}$.

Relationships between Epithelial Permeability and PSA_d. There was wide variability in the cell monolayer permeability coefficients of the nine investigated compounds (0.104×10^{-6} to 242×10^{-6} cm/s; Table 2). The resulting relationship between epithelial permeability and $PSA_{d,vacuum}$ for the compounds is shown in Figure 2. The insert shows the correlation between log P_c and $PSA_{d,vacuum}$ ($r^2 = 0.907$, $q^2 = 0.810$, $n = 9$). If H 216/44 is excluded from the data set, the correlation is slightly improved ($r^2 = 0.968$, $q^2 = 0.942$, $n = 8$; the dashed line in the Figure 2 insert), indicating a stronger relationship for compounds that are more similar structurally. For compounds **B**−**I**, the relationships between P_c and PSA_d resulting from the different solvation models were not qualitatively different; they appeared rather to be only slightly shifted along the PSA_d axis (Figures 2 and 3, Table 4). When H 216/44 was included in the data set, however, a weaker relationship was obtained between $PSA_{d,chloroform}$ and P_c than between $PSA_{d,vacuum}$ and P_c. In contrast, the relationship between $PSA_{d,water}$ and P_c was unaffected by the inclusion of H 216/44 (Table 4, Figure 3).

PSA_d and log D_{calc} in Predictions of Caco-2 Cell Monolayer Permeability. As expected, the three analogues, practolol, H 95/71, and H 244/45, displayed comparable polar surface areas: $PSA_{d,vacuum}$ ranged from 71.6 to 77.0 Å^2 (Table 2). The calculated octanol/water distribution coefficients were similar for H 95/71 and practolol, but a higher lipophilicity, comparable to that of pindolol and metoprolol, was predicted for H 244/45 from these calculations. However, the measured log D values of the three analogues were of the same magnitude (Table 2). Thus, in this case, the

Table 2. Physicochemical Properties, Structural Descriptors, and Caco-2 Cell Monolayer Permeability Coefficients of the β-Adrenoreceptor Antagonists

compound	$PSA_{d,vacuum}$ (Å^2)	$PSA_{d,chloroform}$ (Å^2)	$PSA_{d,water}$ (Å^2)	$SA_{d,vacuum}$ (Å^2)	log D_{calc}	log D_m	log K_s[b] (M^{-1})	P_c[c] (10^{-6} cm/s)
A. H216/44	88.7	70.8	116.6	574.8	−0.61	−0.10[a]	1.09	0.104 ± 0.016
B. atenolol	90.9	91.6	92.6	370.4	−2.31	−2.04[a]	0.37	1.02 ± 0.10
C. H95/71	77.0	77.7	77.7	347.8	−1.34	−1.56	0.62	3.75 ± 0.34
D. practolol	73.4	74.3	74.1	372.3	−1.35	−1.31[a]	0.72	3.46 ± 0.53
E. H244/45	71.6	72.7	72.9	396.9	−0.82	−1.08	0.68	6.03 ± 0.26
F. pindolol	56.5	57.4	57.5	340.7	−0.63	−0.55[a]	1.61	54.7 ± 0.6
G. metoprolol	53.2	53.9	53.9	395.4	−1.11	−0.42[a]	1.15	91.9 ± 4.0[d]
H. oxprenolol	46.7	49.1	49.6	373.4	−0.41	0.08[a]	1.63	119.6 ± 6.7
I. alprenolol	37.1	38.6	39.1	365.4	0.40	0.85[a]	2.44	242 ± 14[d]

[a] From ref 46. [b] $n = 3$; relative SD ≤ 10%. [c] $n = 6-8$. [d] From ref 18.

Table 3. Predicted Caco-2 Cell Monolayer Permeability Coefficients of the Two Practolol Analogues, H 95/71 and H 244/45, and H 216/44 from Relationships between Structural Descriptors and log P_c Derived from Data of the Six Original Model Drugs[a]

	predicted P_c from linear model (10^{-6} cm/s) (predicted P_c/experimental P_c)			predicted P_c from sigmoidal model (10^{-6} cm/s) (predicted P_c/experimental P_c)		
	H 95/71	H 244/45	H 216/44	H 95/71	H 244/45	H 216/44
experimental P_c	3.75	6.03	0.104	3.75	6.03	0.104
$PSA_{d,vacuum}$[b]	4.39	7.87	1.23	2.40	4.56	1.09
	(1.2)	(1.3)	(12)	(0.64)	(0.76)	(10)
$PSA_{d,chloroform}$[c]	4.41	7.67	9.54	2.42	4.35	5.74
	(1.2)	(1.3)	(92)	(0.65)	(0.72)	(55)
$PSA_{d,water}$[d]	4.66	7.93	0.065	2.39	4.16	0.74
	(1.2)	(1.3)	(0.6)	(0.64)	(0.69)	(7)
log D_{calc}[e]	11.6	34.0	53.3	4.24	116	117
	(3.1)	(5.6)	(512)	(1.1)	(19)	(1125)
log K_s[f]	4.61	5.40	15.8	1.70	2.52	66.6
	(1.2)	(0.9)	(152)	(0.45)	(0.42)	(640)

[a] Original model drugs: atenolol, practolol, pindolol, metoprolol, oxprenolol, and alprenolol.[18] [b] log $P_c = 4.274-0.047 \times PSA_{d,vacuum}$ ($r^2 = 0.964$, $n = 6$). [c] log $P_c = 4.390-0.048 \times PSA_{d,chloroform}$ ($r^2 = 0.967$, $n = 6$). [d] log $P_c = 4.385-0.048 \times PSA_{d,water}$ ($r^2 = 0.964$, $n = 6$). [e] log $P_c = 2.283 + 0.912 \times$ log D_{calc} ($r^2 = 0.805$, $n = 6$). [f] log $P_c = -0.042 + 1.139 \times$ log K_s ($r^2 = 0.808$, $n = 6$).

Table 4. Resulting r^2, q^2, and RMSE Values from Fitting Linear or Sigmoidal Models to the Structure−log P_c Data[a]

	linear model			sigmoidal model[b]		
descriptor	r^2	q^2	RMSE	r^2	q^2	RMSE
$PSA_{d,vacuum}$	0.968/0.907	0.942/0.810	0.17/0.36	0.993/0.926	0.966/0.722	0.09^{ns}/0.38^{ns}
$PSA_{d,chloroform}$	0.971/0.650	0.944/0.495	0.16/0.70	0.995/0.787	0.980/0.475	0.08^{ns}/0.65^{ns}
$PSA_{d,water}$	0.967/0.979	0.936/0.965	0.17/0.17	0.995/0.988	0.980/0.861	0.08^{ns}/0.15^{ns}
log D_{calc}	0.725/0.269	0.613/< 0	0.49/1.01	0.746/0.286	<0/<0	0.58^{ns}/1.18^{ns}
log K_s	0.840/0.485	0.644/0.324	0.38/0.85	0.948/0.774	0.768/< 0	0.26^{ns}/0.67^{ns}

[a] Data from regression analyses excluding/including H 216/44 in the data set are presented. [b] ns, not significantly improved fit compared to linear model ($p > 0.05$, F-test for equality of variances).

fragmental method used to calculate log D exaggerated the difference in lipophilicity between the analogues. From the linear relationship between $PSA_{d,vacuum}$ and log P_c of the original model drugs (atenolol, practolol, pindolol, metoprolol, oxprenolol, and alprenolol in ref 18), the cell monolayer permeability to H 95/71 and H 244/45 was predicted to be 4.39×10^{-6} and 7.87×10^{-6} cm/s, respectively (Table 3). This was in good agreement with the observed P_c values of 3.75×10^{-6} and 6.03×10^{-6} cm/s, respectively (Table 2). The P_c values predicted from the $PSA_{d,chloroform}$ and $PSA_{d,water}$ of H 95/71 and H 244/45 were similar (Table 3). However, when the corresponding relationship between log D_{calc} and log P_c was used, epithelial permeabilities to H 95/71 and H 244/45 were overestimated, with predicted P_c values of 11.6×10^{-6} and 34.0×10^{-6} cm/s, respectively (Table 3).

The cell monolayer permeability to H 216/44 was not as well-predicted from the log P_c vs $PSA_{d,vacuum}$ relationship as those of H 95/71 and H 244/45. From $PSA_{d,vacuum}$ = 88.7 Å^2 for H 216/44, a P_c value of 1.23×10^{-6} cm/s was predicted (Table 3). This is about 12-fold higher than the observed cell monolayer permeability ($0.104 \pm 0.016 \times 10^{-6}$ cm/s). In contrast to H 95/71 and H 244/45, the P_c value of H 216/44 predicted from the data of the original model drugs was dependent on the solvation environment of the conformational analysis. Thus, the predicted P_c of H 216/44 from $PSA_{d,chloroform}$ was 9.54×10^{-6} cm/s as compared to 0.065×10^{-6} cm/s from $PSA_{d,water}$ (Table 3). This clearly demonstrates the influence of conformational preferences on the polar surface properties of large, flexible molecules with several functional groups that can participate in hydrogen bonding. However, further studies are needed before it can be stated that the molecular surface properties in a water environment better describe the epithelial permeability.

log D_{calc} was inferior to PSA_d (independent of solvation treatment) as a descriptor of the epithelial transport of H 216/44, predicting a P_c of 53.3×10^{-6} cm/s, or 500-fold higher than that observed (Table 3). The relationship between log D_{calc} and Caco-2 permeability is shown in Figure 4. Inclusion of H 216/44 abolished the correlation between log D_{calc} and log P_c (from $r^2 = 0.725$, $q^2 = 0.613$, $n = 8$ to $r^2 = 0.269$, $q^2 < 0$, $n = 9$). This result cannot be attributed to the theoretical approach

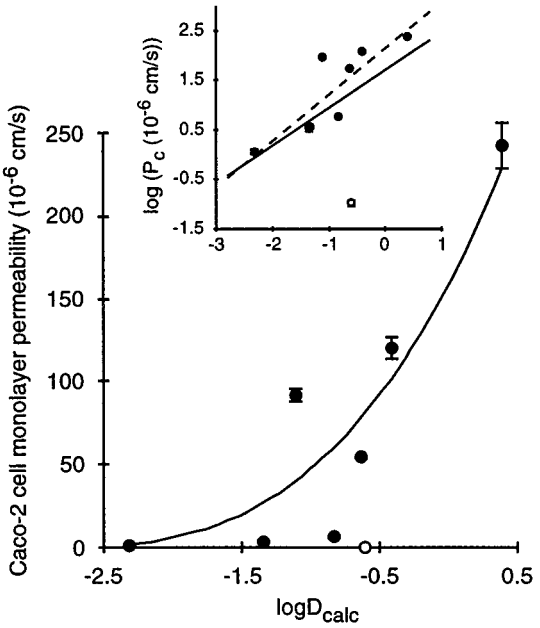

Figure 4. Relationship between log D_{calc} of the nine compounds and their Caco-2 cell monolayer permeability coefficients. The insert shows the correlation between log P_c and log D_{calc}. The dashed line shows the resulting linear correlation when H 216/44 (open circle) is excluded from the data set. Error bars represent SD of P_c.

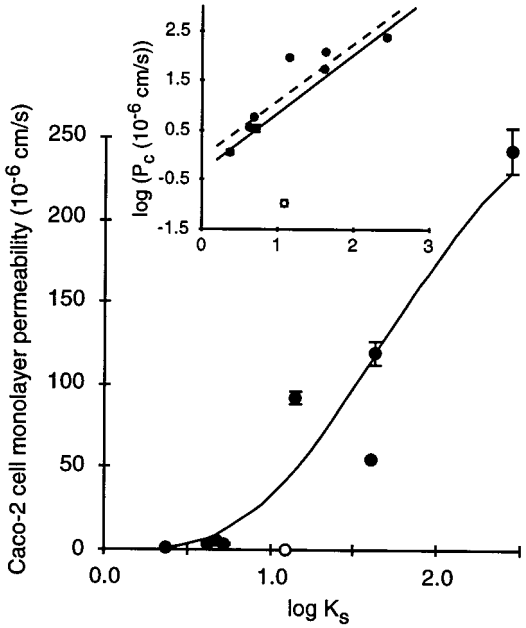

Figure 5. Relationship between log K_s of the nine compounds and their Caco-2 cell monolayer coefficients. The insert shows the correlation between log P_c and log K_s. The dashed line shows the resulting linear correlation when H 216/44 (open circle) is excluded from the data set. Error bars represent SD of P_c.

of calculating the distribution coefficient since the measured log *D* value (log D_m) of H 216/44 at pH 7.4 is close to the calculated value. The log D_m value of H 216/44 is similar to those of metoprolol and oxprenolol (Table 2). However, these compounds permeate Caco-2 cell monolayers approximately 1000 times more easily than H 216/44. This illustrates that single physicochemical predictors are often insufficient to describe the structure−permeability relationship of a more heterogeneous set of compounds (see below).

The predictions of epithelial permeability cited above have been made assuming a linear relationship between the structural descriptors and log P_c. The relationships between the logarithm of the transport rate and structural descriptors such as lipophilicity are, however, often reported to be sigmoidal[1,29] or, when very lipophilic compounds are included, parabolic.[30] In the sigmoidal relationship, the lower plateau represents the paracellular permeability, which is an aqueous pathway. In the present study, no clear evidence of a lower plateau was observed in the investigated permeability range. The upper plateau is often attributed to the limiting effect of the aqueous boundary layer on drug diffusion in vitro.[31] In this study, cell monolayer permeabilities unbiased by the aqueous boundary layer were used, and an upper plateau was therefore not evident. Fitting a four-parameter sigmoidal model to the data did not significantly improve any of the studied structure−absorption relationships (Table 4). Similarly, no improvement was obtained in the prediction of monolayer permeability to H 95/71, H 244/45, and H 216/44 from relationships obtained with the original set of model drugs[18] (Table 3).

Apart from hydrogen bonding and lipophilicity, the charge and the size of molecules can also influence their transepithelial transport. These factors are not included in the PSA_d parameter. log *D*, however, does account for the charge of the compounds. The unexpectedly low permeability of H 216/44 cannot be explained by charge, since this compound is predicted to be charged to a lesser extent at pH 7.4 than the other compounds (pK_a 8.5 compared to pK_a 9.5−9.7 for all other compounds). Instead, the larger size of H 216/44 (MW 479 compared to MW 248−267; SA_d 575 Å^2 compared to SA_d 341−397 Å^2) could in part explain its low epithelial transport.[32] First, it has been proposed that the permeability of a membrane to molecules is directly proportional to the diffusion coefficient of the molecules[33] and subsequently to 1/(molecular volume)^n.[34] Second, assuming that molecular weight is proportional to molecular volume, epithelial permeability has been corrected for molecular size using factors such as MW$^{1/3}$,[35] MW,[1,10] and MW$^{1.4}$.[36] Accordingly, the larger size of H 216/44 compared to the other compounds would account for a 1.3−2.5-fold size-dependent reduction in P_c. Thus, the molecular size of H 216/44 only provides a marginal contribution to the 1000-fold lower cell monolayer permeability to H 216/44 compared to the other compounds of comparable lipophilicity. Instead, it is more likely that the hydrogen-bonding/polar properties of H 216/44 explain most of its limited epithelial transport.

Immobilized Liposome Chromatography. The relationship between specific capacity factor on ILC columns (log K_s) and Caco-2 cell monolayer permeability was not as strong as those between the PSA_d descriptors and P_c (Figure 5). Practolol and the two analogues, H 95/71 and H 244/45, displayed comparable retention properties on the ILC columns (Table 2). As for PSA_d, the predicted cell monolayer permeabilities of H 95/71 and H 244/45 (obtained from the correlation between log K_s and log P_c of the original model drugs) were in good agreement with the P_c values determined experimentally (Table 3). However, log K_s of H 216/44

predicted a P_c value of 15.8×10^{-6} cm/s, which is about 150-fold higher than that observed. When H 216/44 was included in the data set, the relationship between log P_c and log K_s weakened significantly (from $r^2 = 0.840$, $q^2 = 0.644$, $n = 8$ to $r^2 = 0.485$, $q^2 = 0.324$, $n = 9$; Figure 5 and Table 4). Similar results were obtained by fitting a sigmoidal model to the data (Table 4). It is possible that better relationships can be obtained after optimization of the phospholipid composition of the immobilized liposomes.[40] The retention on membrane mimicking chromatographic columns has previously been shown to be closely correlated to log D.[37] Also in this study, log K_s was strongly correlated to experimentally determined log D values (log D_m, Table 2; $r^2 = 0.92$). However, the relationship between log K_s and log P_c was somewhat stronger than that between log D_m and log P_c when H 216/44 was included.

In contrast to PSA_d, log K_s is expected to account for the distribution of charged and uncharged species since it is measured at the pH of the transport experiments. However, the influence of charge on the retention on membrane-like columns is unclear. It has been shown that retention on IAM columns decreases with ionization of acidic groups but is not affected by the ionization of basic groups.[38] Further, distribution of ion pairs into liposomes has been suggested to decrease the effects of molecular charge on liposome partitioning.[39]

The ILC retention of a solute results from a combination of electrostatic interactions with the bilayer surface, partitioning into the lipid bilayer and partitioning into the interior of the immobilized liposomes. Although electrostatic interactions are weak for small solutes at physiological ionic strength,[40] a large hydrogen-bonding capacity will not necessarily prohibit an interaction with the lipid bilayer surface and subsequent retention on the ILC column. For example, peptides have been shown to be able to remain solvated at the membrane interface.[41] Thus, retention on an ILC column will not always reflect transport across a cell membrane. This might explain the discrepancy between the retention on ILC columns and cell monolayer permeability found in this study, especially for H 216/44, and the stronger relationships obtained with the PSA_d descriptors.

Conclusions

The results of this study provide further support for the hypothesis that molecular surface properties determine cell membrane permeability and, hence, epithelial permeability to drug molecules. More specifically, the molecular descriptor PSA_d, which is related to the hydrogen-bonding capacity, was found to be a good predictor of the intestinal epithelial permeability to an analogous series of β-receptor-blocking agents. In general, the influence on PSA_d of using simulated solvent environments in conformational analyses was small. Good correlations between PSA_d and P_c were established in all environments (vacuum, water, and chloroform). The exception was H 216/44 which is an outlier with regard to molecular properties. H 216/44 is a larger and more flexible molecule capable of forming several intra- and intermolecular hydrogen bonds. The P_c of H 216/44 was excellently predicted by the PSA of the extended conformation preferred in the simulated water environment. The PSA_d obtained in chloroform overestimated the P_c of H 216/44 92-fold. Including H 216/44 in the data set weakened the correlation between $PSA_{d,chloroform}$ and P_c dramatically. These results indicate that while single molecular descriptors such as PSA_d may be good predictors of epithelial permeability to series of drug molecules with limited structural differences, they may be insufficient for drugs of greater structural diversity. However, in all cases, PSA_d was a better predictor of drug transport across the intestinal epithelium than calculated log D values or experimentally determined log K_s values obtained using immobilized liposome chromatography. These results motivate further studies on how PSA_d and other molecular surface properties determine membrane permeability for structurally different drugs.

Experimental Section

Synthesis of H 95/71. *N*-(4-Hydroxyphenyl)formamide (1). 4-Aminophenol (49.1 g, 0.45 mol) was dissolved in formic acid (337.5 mL). The solution was heated to reflux for 1 h and was then allowed to cool to room temperature. The formic acid was evaporated off. The residue was partitioned between EtOAc (500 mL) and 2 M HCl (250 mL). The organic phase was washed with 2 M HCl (250 mL), H_2O (250 mL), and brine (250 mL) and dried ($MgSO_4$). Evaporation of the volatiles gave 40 g (64.8%) of **1** as a solid. Mp: 138−139 °C. Compound **1** was used in the next step without further purification.

***N*-[4-(2,3-Epoxypropoxy)phenyl]formamide (3).** KOH (5.8 g, 90.7 mmol) was dissolved in H_2O (150 mL), and compound **1** (15 g, 90.7 mmol) was added. Epichlorohydrin (8.81 g, 95.2 mmol) was thereafter added dropwise to the dark solution. The mixture was stirred at room temperature for 6 h. EtOAc (300 mL) was added, and the phases were separated. The organic phase was washed with H_2O (200 mL) and brine (100 mL). After drying ($MgSO_4$) the volatiles were evaporated off. The residual brownish oil was purified by column chromatography on silica gel using heptane/EtOAc (3:2) as eluent to afford 8.0 g (45.6%) of **3**. Compound **3** was used in the next step without further purification.

***N*-[4-(2-Hydroxy-3-(isopropylamino)propoxy)phenyl]-formamide (H 95/71).** Compound **3** (8.0 g, 41.4 mmol) and 2-propylamine (3.55 mL, 41.4 mmol) were dissolved in EtOH (30 mL) in a sealed glass ampule. The mixture was stirred at 100 °C for 2 h and was then allowed to cool to room temperature. The volatiles were evaporated off. The residue was purified by column chromatography on silica gel using CH_2Cl_2/MeOH/NH_3(aq) (10:1.5:0.15) as eluent to afford 2.9 g (27.8%) of pure product. Mp: 121−122 °C. ^{1}H NMR (270 MHz) ($CDCl_3$) (1:1 mixture of amide rotamers): δ 8.49 (br s, 0.5H), 8.34 (d, 0.5H, $J = 1.7$ Hz), 7.43 (d, 1H, $J = 9.0$ Hz), 7.01 (d, 1H, $J = 9.0$ Hz), 6.91 (d, 1H, $J = 8.8$ Hz), 6.88 (d, 1H, $J = 9.0$ Hz), 4.12−4.01 (m, 1H), 3.96−3.98 (m, 2H), 2.96−2.71 (m, 5H), 1.13 (dd, 6H, $J = 6.37$, 1.64 Hz). Anal. Calcd. for $C_{13}H_{20}N_2O_3$: C, 61.8; H, 8.0; N, 11.2. Found: C, 61.6; H, 7.7; N, 11.0.

Synthesis of H 244/45. *N*-(4-Hydroxyphenyl)propionamide (2). Propionic anhydride (33.1 g, 0.254 mol) was added to a suspension of 4-aminophenol (21.8 g, 0.2 mol) in H_2O (60 mL). A homogeneous solution was obtained after heating to reflux for 10 min. A precipitate was formed when the solution was allowed to cool to room temperature. The precipitate was filtered off and washed with 4 × 75 mL of H_2O. The white solid was dried in vacuo over P_2O_5 to obtain 29.8 g (90.2%) of **2**. Compound **2** was used in the next step without further purification.

***N*-[4-(2,3-Epoxypropoxy)phenyl]propionamide (4).** KOH (11.5 g, 0.18 mol) was dissolved in H_2O (300 mL). Compound **2** (29.8 g, 0.18 mol) was added, and a clear solution was obtained after a few minutes. Epichlorohydrin was added dropwise. A white precipitate was observed after ca. 30 min. The mixture was stirred overnight at room temperature. The solid material was filtered off, washed with 4 × 100 mL H_2O,

and dried in vacuo over P_2O_5 to obtain 38.2 g (95.9%) of **4**. Compound **4** was used in the next step without further purification.

***N*-[4-(2-Hydroxy-3-(isopropylamino)propoxy)phenyl]-propionamide (H 244/45).** Compound **4** (15.0 g, 67.8 mmol) and 2-propylamine (5.8 mL, 67.8 mmol) were dissolved in EtOH (40 mL) in a sealed glass ampule. The mixture was stirred at 100 °C for 2 h and was then allowed to cool to room temperature. The volatiles were evaporated off. Dry diethyl ether (300 mL) was added to the residue to obtain a white solid which was filtered off. Purification by column chromatography on silica gel using CH_2Cl_2/MeOH/NH_3(aq) (10:1:0.1) as eluent afforded 9.5 g (50.0%) of pure product. Mp: 135−138 °C. ^{1}H NMR (270 MHz) ($CDCl_3$): δ 7.39 (d, 2H, J = 8.9 Hz, H2′, H2″), 7.11 (br s, 1H, amide NH), 6.86 (d, 2H, J = 8.9 Hz, H3′, H3″), 4.02 (m, 1H, H2), 3.95 (app d, 2H, H1), 2.91 (dd, 1H, J = 3.66, −11.96 Hz, H3a), 2.87 (hept, 1H, J = 6.35 Hz, NC*H*), 2.74 (dd, 1H, J = 7.90, −11.96 Hz, H3b), 2.54 (br s, 2H, NH, OH), 2.37 (q, 2H, J = 7.57 Hz, CH_3CH_2), 1.24 (t, 3H, J = 7.57 Hz, CH_3CH_2), 1.12 (d, 6H, J = 6.35, $CHCH_3$). Anal. Calcd. for $C_{15}H_{24}N_2O_3 \cdot 0.1H_2O$: C, 63.8; H, 8.6; N, 9.9. Found: C, 63.8; H, 8.5; N, 9.8.

Calculation of Molecular Surface Properties. A. Conformational Analysis. Conformational analyses of all nine β-receptor-blocking agents (see Table 1) were performed by molecular mechanics calculations, using the MM2 force field as implemented in the MacroModel program (v 4.5).[42] Systematic pseudo-Monte Carlo conformational search procedures were used for each compound in vacuum, simulated chloroform, and simulated water environments.

Two to four 5000-step conformational searches were carried out in each environment. Starting structures with two different configurations of the amino group and when appropriate *cis*- and *trans*-conformations of amide groups were used. The energy window was set to 7 kcal/mol. Energy minimizations were made using the truncated Newton algorithm, a maximum of 3000 iterations, and a convergence criterion of 0.01 kJ/Å·mol. The conformational analysis of H 216/44 in vacuum was performed using 100 000 steps in order to account for the extensive conformational freedom of this molecule. Since the calculations took considerably longer in simulated chloroform and water environments than in vacuum, it was not possible to analyze the conformational space of H 216/44 as exhaustively in these environments. Six different starting conformations were used in 5000-step searches in simulated chloroform. A similar procedure was used for calculations in simulated water, but because the calculations were even slower in this environment, nine different starting conformations and 1000 steps were used.

For all compounds, an additional energy minimization with a lower convergence criterion (0.001 kJ/Å·mol) was performed on the resulting conformations from all searches. The conformations of each compound were then combined, and duplicate conformers were removed. Only the (*S*)-enantiomers were considered, since enantiomers have identical surface properties.

B. Dynamic Surface Area Calculations. The van der Waals' surface areas of all low-energy conformations ($\Delta E_s \leq$ 2.5 kcal/mol) of the nine investigated compounds were calculated using an in-house program. The analytical algorithm was developed to reduce the effect of spatial orientation found in numerical calculations and to increase speed and precision in the surface area calculations. The program calculates the free surface area of each atom bounded by the arcs of the overlapping atoms using the Gauss−Bonnet theorem.[43] The molecular surface area was divided into a polar fraction (nitrogen atoms, oxygen atoms, and hydrogen atoms attached to these heteroatoms) and a nonpolar fraction. The dynamic averages of the surface properties were then calculated from all low-energy conformations according to a Boltzmann distribution at 37 °C.[17,18]

C. Calculation of Octanol/Water Distribution Coefficients. The logarithms of the octanol/water partition coefficients (log *P*) for the nine investigated compounds were calculated according to the method by Hansch and co-workers[44] using CLOGP v 4.42 (Daylight C.I.S. Inc., Irvine, CA). The distribution coefficients at pH 7.4 (log *D*) were computed from the CLOGP values and experimentally determined pK_a values.[45,46]

D. pK_a and Octanol/Water Distribution Coefficient Measurements. The octanol/water partition coefficients of H 95/71 and H 244/45 were determined experimentally using a titrimetric method. For all other compounds experimentally determined values of log *D* (log D_m) were taken from literature.[46] The apparatus, a Sirius PC101 pK_a and log *P* analyzer (Sirius Analytical Instruments Ltd., Forest Row, England), was equipped with an Orion Ross semimicro combination pH electrode (model 8103SC, ATI Orion, Boston, MA). The titration vessel was a closed system containing an electrode, a stirrer, a temperature probe, a precision dispenser, and a tube for introduction of nitrogen gas. Separate titrations were performed to estimate pK_a in water and the apparent pK_a in the presence of *n*-octanol (pK_a') in a two-phase system of water and *n*-octanol. The difference between pK_a and pK_a' is related to log *P*.[47] Weighed samples of H 95/71 and H 244/45 (1−2 mg), and 1.0 mL of *n*-octanol in the pK_a' titrations, were added to a vial before it was placed into the temperature-controlled vessel (25 °C). Water adjusted for ionic strength (0.15 M KCl; 10−15 mL) was added, and the solutions were acidified with 0.5 M HCl to a pH of 2. The mixture was stirred until all of the sample was dissolved. Titrations were performed under a nitrogen blanket with 0.5 M KOH as titrant up to pH 11. To obtain the equilibrium constants, nonlinear regression analysis of the difference curves[47] was performed on the data sets using the pK_a LOGP software (v 4.0; Sirius Analytical Instruments).

Drug Transport Studies. A. Cell Culture. Caco-2 cells were obtained from American Type Culture Collection (Rockville, MD). The cells were maintained in Dulbecco's modified Eagle's medium (DMEM), containing 10% heat-inactivated fetal calf serum (FCS) and 1% nonessential amino acids, in an atmosphere of 90% air and 10% CO_2 as described elsewhere;[48] 5×10^5 cells (passage number 93−105) were seeded on polycarbonate filter inserts (Transwell Costar, Badhoevedorp, The Netherlands; mean pore size 0.45 μm, diameter 12 mm) and cultivated in DMEM supplemented with 10% FCS, 1% nonessential amino acids, penicillin (100 units/mL), and streptomycin (100 μg/mL).[23] All tissue culture media were obtained from Gibco through Laboratorie Design AB, Lidingö, Sweden. The cells were allowed to grow and differentiate for 22−32 days before the monolayers were used in drug transport experiments.

B. Drug Transport Experiments. In general, drugs were dissolved in Hanks' balanced salt solution containing 25 mM Hepes buffer (HBSS; pH 7.4) to a final concentration of 1−2 mM. In addition, H 216/44 was used also at 5 mM in order to saturate active transport processes (see below). The drug solutions (pH 7.4) were added to the donor side of the monolayers, and HBSS without drug was added to the receiver side. The monolayers were incubated at 37 °C in a humidified atmosphere. At regular time intervals (4−40 min depending on transport rate) samples were withdrawn from the receiving chamber and frozen (−20 °C) pending HPLC analysis. A calibrated plate shaker was used to agitate the monolayers, and transport experiments were carried out at both low- and high-stirring rates.[31] The integrity of the monolayers was routinely checked by determination of their permeability to the hydrophilic marker [^{14}C] mannitol.[49] The baseline apparent permeability of mannitol was $0.12 \pm 0.04 \times 10^{-6}$ cm/s (n = 67). No significant effect on integrity was observed at the drug concentrations and stirring rates used, compared to control experiments. The transport rates were also determined in both apical-to-basolateral (a−b) and basolateral-to-apical (b−a) directions in order to detect any significant active transport of the compounds.

In general, the P_c ratio (b−a)/(a−b) was in the vicinity of 1, indicating that the prevailing transport mechanism was passive diffusion. However, a (b−a)/(a−b) ratio of approximately 30 was observed for H 216/44 at 1 mM,[50] which was

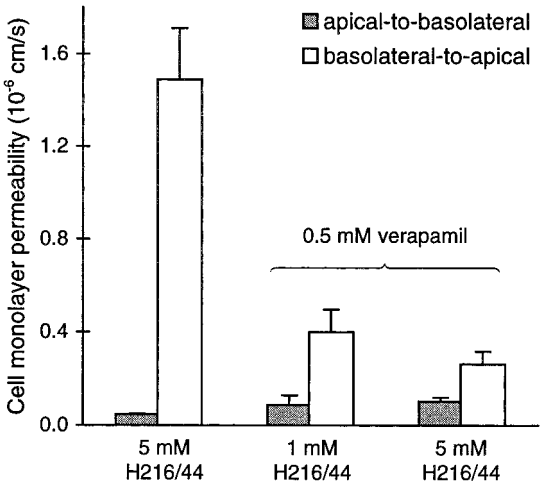

Figure 6. Transport of H 216/44 across Caco-2 cell monolayers in the apical-to-basolateral and basolateral-to-apical directions in the absence or presence of the P-glycoprotein substrate verapamil (0.5 mM). Error bars represent SD of P_c.

taken as an indication of a significant active secretory component.[51,52] To obtain a better estimate of the passive absorption component, Caco-2 permeability to H 216/44 was also measured at a higher drug concentration (5 mM), with or without addition of 0.5 mM verapamil, an inhibitor of P-glycoprotein-mediated secretion[52] (Figure 6). Increasing the concentration of H 216/44 to 5 mM without verapamil did not reduce the (b−a)/(a−b) ratio.[53] However, after addition of verapamil, the (b−a)/(a−b) ratio decreased from 32 to 2.5, which was comparable to that of practolol. Consequently, the apical-to-basolateral Caco-2 cell monolayer permeability coefficient of H 216/44 measured at 5 mM in the presence of 0.5 mM verapamil apically was used in the analysis of structure−absorption relationships.

C. Analytical Methods. The samples from the drug transport studies were analyzed using a reversed-phase HPLC system. The system consisted of a Perkin-Elmer isocratic LC pump 250, a Perkin-Elmer advanced LC sample processor ISS-200, and a Spectra Physics UV100 detector. The integration software Chromatography Station for Windows was used in the analysis of H 216/44. For all other compounds a Spectra Physics SP4270 integrator was used. A Hichrom Partisil ODS3 (100 × 4.6 mm) was used as analytical column and a Hichrom Partisil ODS3 (10 × 3.2 mm) was used as guard column, both with a mean particle size of 5 μm, for all compounds but H 216/44. The analytical column used in the analysis of H 216/44 was a Beckman Ultrasphere ODS (250 × 4.6 mm) with a particle size of 5 μm. The mobile phase was composed of phosphate buffer (pH 3.0; 60 mM KH_2PO_4, 8 mM H_3PO_4) and acetonitrile; 10−30% acetonitrile was used to obtain retention times of 3−12 min at flow rates of 0.5−1.0 mL/min. Injection volumes were 10 to 200 μL. Samples containing [^{14}C]mannitol were counted in a liquid scintillation spectrometer (Tricarb 1900 CA, Packard Instruments).

D. Permeability Coefficients. All rate constants were obtained under "sink" conditions (i.e., the concentration of the drug on the receiver side never exceeded 10% of the concentration of the drug on the donor side), and the mass balance was checked at the end of all transport experiments. The observed mass balance was in general >95% and never <85%. The apparent permeability coefficient (P_{app}, cm/s) was calculated from:

$$P_{app} = (k \cdot V_R)/(A \cdot 60) \quad (1)$$

where k is the slope obtained by linear regression of cumulative fraction absorbed as a function of time (min), V_R is the volume in the receiver chamber (mL), and A is the area of the membrane (cm^2). The fraction absorbed was defined as the ratio between the concentration on the receiver side at the end of an interval and the concentration on the donor side at the beginning of that interval. The cell monolayer permeability (P_c), unbiased by the aqueous boundary layer, was calculated from the relationship between P_{app} determined at the different stirring rates (V) and V, as described previously:[31]

$$V/P_{app} = 1/K + (1/P_c + 1/P_f) \cdot V \quad (2)$$

where P_f is the calculated permeability coefficient of the filter support and K is a constant.

Immobilized Liposome Chromatography. A. Preparation and Immobilization of Liposomes. Superdex 200 (preparative grade) and a glass column (HR 5/5) were bought from Pharmacia Biotech (Uppsala, Sweden) and phosphatidylcholine (PC; hens' egg, 95% purity) was obtained from Avanti Polar Lipids (Alabaster, AL). Chemicals were of analytical grade. The procedures for liposome immobilization and drug retention analysis were essentially as described earlier.[11] In brief, liposomes (1.5 mL, 150 μmol of phospholipid), prepared by rehydration of a PC film in 150 mM NaCl, 1 mM Na_2EDTA, and 10 mM Tris-HCl, pH 7.4, were mixed with dried Superdex 200 gel beads (110 mg) and were immobilized by gel bead swelling followed by freezing and thawing to effect liposome fusion.[54,55] The material was packed in the 5-mm (i.d.) glass column to a 1.0-mL gel bed. Phosphorus analysis showed 47.6 μmol of phospholipid before packing and 43.9 μmol after the runs.[55] The average value was used in eq 3 below.

B. Chromatographic Procedure. The mobile phase consisted of 150 mM NaCl in 10 mM sodium phosphate buffer, pH 7.4. Aliquots of the nine investigated drugs in the eluent (10−50 μL, 0.1 mg/mL) were analyzed at 0.80 ± 0.02 mL/min at 23 °C with detection at 220 nm.

C. Specific Capacity Factor (K_s). The capacity factor, K_s, for a drug was calculated using

$$K_s = (V_R - V_0)/A \quad (3)$$

where V_R is the retention volume of the drug which was read at the peak maximum, V_0 is the retention volume of the reference substance ($K_2Cr_2O_7$), and A is the amount of immobilized phospholipid (see above). The units were chosen to obtain K_s in M^{-1}.

D. Statistical Analysis. Values are given as mean ± one standard deviation (SD). Unpaired Student's t-test or ANOVA, when appropriate, was used to determine statistical differences between mean values. Variances were compared using Scheffe's F-test. $P < 0.05$ was considered as significant. The coefficient of determination (r^2), the (leave-one-out) cross-validated r^2 (q^2), and the root-mean-square error (RMSE) were used as measures of goodness-of-fit in regression analyses. The sum of squared residuals was minimized in nonlinear regression analyses to fit the four-parameter sigmoidal equation:

$$y_{calc} = (y_{max} - y_{min})/(1 + (x/x_{50})^{\gamma}) + y_{min} \quad (4)$$

to the data, where x is the structural property (PSA_d, log D, or log K_s), x_{50} is the value of x at $y_{min} + (y_{max} - y_{min})/2$, and γ is a slope factor. When the permeability data were not logarithmically transformed, a weighting scheme of $1/y_{calc}^2$ was used in the regression analyses.

Acknowledgment. We would like to thank Magnus Köping-Höggård for skillful assistance with the transport experiments and Johan Gråsjö for valuable mathematical assistance. This work was supported by Grant 97-46 from Centrala Försöksdjursnämnden, Grant 9478 from The Swedish Medical Research Council, Grant K11163-302 from The Swedish Natural Science Research Council, and The Swedish Fund for Scientific Research without Animals.

Supporting Information Available: Table of results from the conformational analyses and surface area calculations (1 page). Ordering information is given on any current masthead page.

References

(1) Artursson, P.; Karlsson, J. Correlation between oral drug absorption in humans and apparent drug permeability coefficients in human intestinal epithelial (Caco-2) cells. *Biochem. Biophys. Res. Commun.* **1991,** *175,* 880−885.

(2) Lennernäs, H.; Palm, K.; Fagerholm, U.; Artursson, P. Comparison between active and passive drug transport in the human intestinal epithelial Caco-2 cells in vitro and human jejunum in vivo. *Int. J. Pharm.* **1996,** *127,* 103−107.

(3) Martin, Y. C. A practitioner's perspective of the role of quantitative structure−activity analysis in medicinal chemistry. *J. Med. Chem.* **1981,** *24,* 229−237.

(4) Young, R. C.; Mitchell, R. C.; Brown, T. H.; Ganellin, C. R.; Griffiths, R.; Jones, M.; Rana, K. K.; Saunders, D.; Smith, I. R.; Sore, N. E.; Wilks, T. J. Development of a new physicochemical model for brain penetration and its application to the design of centrally acting H_2 receptor histamine antagonists. *J. Med. Chem.* **1988,** *31,* 656−671.

(5) Schoenwald, R. D.; Huang, H.-S. Corneal penetration behavior of beta-blocking agents I: Physicochemical factors. *J. Pharm. Sci.* **1983,** *72,* 1266−1271.

(6) El Tayar, N.; Tsai, R.-S.; Testa, B.; Carrupt, P.-A.; Leo, A. Partitioning of solutes in different solvent systems: The contribution of hydrogen-bonding capacity and polarity. *J. Pharm. Sci.* **1991,** *80,* 590−598.

(7) Conradi, R. A.; Hilgers, A. R.; Ho, N. F. H.; Burton, P. S. The influence of peptide structure on transport across Caco-2 cells. *Pharm. Res.* **1991,** *8,* 1453−1460.

(8) Conradi, R. A.; Hilgers, A. R.; Ho, N. F. H.; Burton, P. S. The Influence of Peptide Structure on Transport Across Caco-2 Cells. II. Peptide Bond Modification Which Results in Improved Permeability. *Pharm. Res.* **1992,** *9,* 435−439.

(9) Ong, S.; Qiu, X.; Pidgeon, C. Solute interactions with immobilized artificial membranes. *J. Phys. Chem.* **1994,** *98,* 10189−10199.

(10) Pidgeon, C.; Ong, S.; Liu, H.; Qiu, X.; Pidgeon, M.; Dantzig, A. H.; Munroe, J.; Hornback, W. J.; Kasher, J. S.; Glunz, L.; Szczerba, T. IAM chromatography: an in vitro screen for predicting drug membrane permeability. *J. Med. Chem.* **1995,** *38,* 590−594.

(11) Beigi, F.; Yang, Q.; Lundahl, P. Immobilized-liposome chromatographic analysis of drug partitioning into lipid bilayers. *J. Chromatogr. A* **1995,** *704,* 315−321.

(12) Amidon, G. L.; Yalkowsky, S. H.; Anik, S. T.; Valvani, S. C. Solubility of nonelectrolytes in polar solvents. V. Estimation of the solubility of aliphatic monofunctional compounds in water using a molecular surface area approach. *J. Phys. Chem.* **1975,** *79,* 2239−2246.

(13) Dunn, W. J., III; Koehler, M. G.; Grigoras, S. The role of solvent-accessible surface area in determining partition coefficients. *J. Med. Chem.* **1987,** *30,* 1121−1126.

(14) Barlow, D.; Satoh, T. The design of peptide analogues for improved absorption. *J. Contr. Relat.* **1994,** *29,* 283−291.

(15) Ooi, T.; Oobatake, M.; Némethy, G.; Scheraga, H. A. Accessible surface areas as a measure of the thermodynamic parameters of hydration of peptides. *Proc. Natl. Acad. Sci. U.S.A.* **1987,** *84,* 3086−3090.

(16) van de Waterbeemd, H.; Kansy, M. Hydrogen-bonding capacity and brain penetration. *Chimia* **1992,** *46,* 299−303.

(17) Lipkowitz, K. B.; Baker, B.; Larter, R. Dynamic molecular surface areas. *J. Am. Chem. Soc.* **1989,** *111,* 7750−7753.

(18) Palm, K.; Luthman, K.; Ungell, A.-L.; Strandlund, G.; Artursson, P. Correlation of drug absorption with molecular surface properties. *J. Pharm. Sci.* **1996,** *85,* 32−39.

(19) Palm, K.; Stenberg, P.; Luthman, K.; Artursson, P. Polar molecular surface properties predict the intestinal absorption of drugs in humans. *Pharm. Res.* **1997,** *14,* 568−571.

(20) The multivariate partial least-squares projections to latent structures (PLS) method was used in: Norinder, U.; Österberg, T.; Artursson, P. Theoretical calculation and prediction of Caco-2 cell permeability using MolSurf parametrization and PLS statistics. *Pharm. Res.* **1997,** *14,* 1785−1790.

(21) Basak, S. C.; Gute, B. D.; Drewes, L. R. Predicting blood-brain transport of drugs: A computational approach. *Pharm. Res.* **1996,** *13,* 775−778.

(22) Lipinski, C. A.; Lombardo, F.; Dominy, B. W.; Feeney, P. J. Experimental and computational approaches to estimate solubility and permeability in drug discovery and development settings. *Adv. Drug Deliv. Rev.* **1996,** *23,* 3−25.

(23) Artursson, P. Epithelial transport of drugs in cell culture. I: A model for studying the passive diffusion of drugs over intestinal absorptive (Caco-2) cells. *J. Pharm. Sci.* **1990,** *79,* 476−482.

(24) This is in contrast with results obtained by NMR spectroscopy in $CDCl_3$ which indicate a 1:1 mixture of amide rotamers in H 95/71. This prevented a more detailed analysis of the spectra due to overlapping peaks. NMR spectra of H 244/45 were more informative indicating preferences for conformations stabilized by intramolecular hydrogen bonding between the amine and alcohol functionalities. No hydrogen bond stabilization involving the ether oxygen was identified. This is in contrast with the results from the Monte Carlo conformational search which gave low-energy conformations including both these hydrogen bonds to about the same extent.

(25) The use of a folded conformation as a starting geometry in a conformational search in simulated water resulted in stretched conformations. The opposite was also observed: using a stretched conformation as starting geometry in simulated chloroform resulted in folded conformations.

(26) The smallest variation in PSA of all low-energy conformations, 11.5 Å^2, was found for pindolol (largest PSA = 61.8 Å^2; smallest PSA = 50.3 Å^2) and the largest variation, 47 Å^2, was displayed by H 216/44 (largest PSA = 116.6 Å^2; smallest PSA = 69.2 Å^2). The low-energy conformations of atenolol identified in chloroform displayed the smallest relative variation in PSA ($\Delta PSA/PSA_d$ = 5.4 Å^2/91.6 Å^2 = 6%), whereas the largest relative variation was found for alprenolol in water ($\Delta PSA/PSA_d$ = 20.9 Å^2/39.2 Å^2 = 54%).

(27) The low-energy conformations were divided into groups according to ref 18. The groups displayed different polar surface properties ($p < 0.001$; ANOVA), and the variation within groups was small.

(28) The polar surface areas reported in this paper differ slightly from those reported in ref 18. In the earlier paper we used the Lee and Richard-based numerical algorithm[57] included in the PCMODEL program (v 4.0), whereas in this paper (as well as in our more recent publication, ref 19) we used an in-house computer program based on an analytical algorithm. In general the polar surface areas calculated with the analytical algorithm were larger (2−4 Å^2) than the numerically calculated areas. This is in agreement with the grid-based numerical algorithm in PCMODEL and the observation that the computed surface areas get larger when a smaller grid size is used in PCMODEL. However, for atenolol and practolol the polar surface areas calculated according to the analytical algorithm were smaller (4−5 Å^2) than the polar areas calculated by PCMODEL. After closer inspection this could be attributed to the fact that the carbon atoms in the carbonyl groups (accounting for approximately 7 Å^2 of the total area) were included in the polar surface area obtained from PCMODEL.

(29) van de Waterbeemd, H.; Camenisch, G.; Folkers, G.; Raevsky, O. A. Estimation of Caco-2 cell permeability using calculated molecular descriptors. *Quant. Struct.-Act. Relat.* **1996,** *15,* 480−490.

(30) Wils, P.; Warnery, A.; Phung-Ba, V.; Legrain, S.; Scherman, D. High lipophilicity decreases drug transport across intestinal epithelial cells. *J. Pharmacol. Exp. Ther.* **1994,** *269,* 654−658.

(31) Karlsson, J.; Artursson, P. A method for the determination of cellular permeability coefficients and aqueous boundary layer thickness in monolayers of intestinal epithelial (Caco-2) cells grown in permeable filter chambers. *Int. J. Pharm.* **1991,** *71,* 55−64.

(32) Depending on whether the epithelial transport is transcellular and/or paracellular, the larger molecular size decreases cell monolayer permeability by either diffusional restriction and/or the sieving effect of the paracellular pathway. The Caco-2 cell monolayer is a relatively tight epithelium with a low paracellular permeability.[2,56] In addition, the active secretion of H 216/44 in the absence of verapamil suggests efflux of H 216/44 across the apical cell membrane of the epithelial cells[52] (see Experimental Section). Thus, one can assume that H 216/44 is to a significant extent transported transcellularly and that the size effect would result from a higher diffusional restriction.

(33) Stein, W. D. The molecular basis of diffusion across cell membranes. *The movement of molecules across cell membranes;* Academic Press: New York, 1967.

(34) The value of n is dependent on the environment. Stokes−Einstein stated a value of 1/3 for spherical molecules. Later experimental values of 0.6−0.7 have been described. For polymers and in lipid bilayers a steeper size dependence has been observed, and values of 1−3 have been assigned to n.[36]

(35) Rubas, W.; Cromwell, M.; Gadek, T.; Narindray, D.; Mrsny, R. Structural elements which govern the resistance of intestinal tissues to compound transport. *Mater. Res. Soc. Symp. Proc.* **1994,** *331,* 179−185.

(36) Xiang, T.-X.; Anderson, B. D. The relationship between permeant size and permeability in lipid bilayer membranes. *J. Membr. Biol.* **1994,** *140,* 111−122.

(37) Barbato, F.; La Rotonda, M. I.; Quaglia, F. Chromatographic indexes on immobilized artificial membranes for local anesthetics: relationships with activity data on closed sodium channels. *Pharm. Res.* **1997,** *14,* 1699−1705.
(38) Salminen, T.; Pulli, A.; Taskinen, J. Relationship between immobilised artificial membrane chromatographic retention and the brain penetration of structurally diverse drugs. *J. Pharm. Biomed. Anal.* **1997,** *15,* 469−477.
(39) Avdeef, A.; Box, K. J.; Comer, J. E. A.; Hibbert, C.; Tam, K. Y. pH-metric logP 10. Determination of liposomal membrane-water partition coefficients of ionizable drugs. *Pharm. Res.* **1998,** *15,* 209−215.
(40) Beigi, F.; Gottschalk, I.; Lagerquist Hägglund, C.; Haneskog, L.; Brekkan, E.; Zhang, Y.; Österberg, T.; Lundahl, P. Immobilized liposome and biomembrane partitioning chromatography of drugs for prediction of drug transport. *Int. J. Pharm.* **1998,** *164,* 129−137.
(41) Jacobs, R. E.; White, S. H. The nature of the hydrophobic binding of small peptides at the bilayer interfaces: implications for the insertion of transbilayer helices. *Biochemistry* **1989,** *28,* 3421−3437.
(42) Mohamadi, F.; Richards, N. G. J.; Guida, W. C.; Liskamp, R.; Lipton, M.; Caufield, C.; Chang, G.; Hendrickson, T.; Still, W. C. MacroModel−An integrated software system for modelling organic and bioorganic molecules using molecular mechanics. *J. Comput. Chem.* **1990,** *11,* 440−467.
(43) The program M-AREA v 1.1 used for surface area calculations is available upon request from the authors (contact johan.grasjo@galenik.uu.se). The program is available free of charge for academic users.
(44) Leo, A.; Jow, P. Y. C.; Silipo, C.; Hansch, C. Calculation of hydrophobic constant (log P) from π and f constants. *J. Med. Chem.* **1975,** *18,* 865−868.
(45) Mannhold, R.; Dross, K. P.; Rekker, R. F. Drug lipophilicity in QSAR practice: I. A comparison of experimental with calculative approaches. *Quant. Struct.-Act. Relat.* **1990,** *9,* 21−28.
(46) Experimentally determined values of pK_a and log D_m were taken from: Craig, P. N. Drug Compendium. In *Cumulative Subject Index & Drug Compendium,* 1st ed.; Drayton, C. J., Ed.; Pergamon Press: Oxford, 1990; pp 237−991; with the exception of pK_a and log D_m of H 216/44: personal communication with Kurt-Jörgen Hoffman, Astra Hässle AB, Sweden.
(47) Avdeef, A. pH-Metric log P. Part 1. Difference plots for determining ion-pair octanol−water partition coefficients of multiprotic substances. *Quant. Struct.-Act. Relat.* **1992,** *11,* 510−517.
(48) Artursson, P.; Karlsson, J.; Ocklind, G.; Schipper, N. Studying transport processes in absorptive epithelia. In *Cell Culture Models of Epithelial Tissues − a Practical Approach;* Shaw, A. J., Ed.; Oxford University Press: New York, 1996; pp 111−133.
(49) Anderberg, E. K.; Nyström, C.; Artursson, P. Epithelial transport of drugs in cell culture. VII: Effects of pharmaceutical surfactant excipients and bile acids on transepithelial permeability in monolayers of human intestinal epithelial (Caco-2) cells. *J. Pharm. Sci.* **1992,** *81,* 879−887.
(50) The receiver concentrations in the a−b direction were close to or below the limit of detection resulting in only approximate permeability values.
(51) Karlsson, J.; Kuo, S.-M.; Ziemniak, J.; Artursson, P. Transport of celiprolol across human intestinal epithelial (Caco-2) cells: mediation of secretion by multiple transporters including P-glycoprotein. *Br. J. Pharmacol.* **1993,** *110,* 1009−1016.
(52) Burton, P. S.; Conradi, R. A.; Ho, N. F. H.; Hilgers, A. R.; Borchardt, R. T. How structural features influence the biomembrane permeability of peptides. *J. Pharm. Sci.* **1996,** *85,* 1336−1340.
(53) Both a−b and b−a epithelial permeability to H 216/44 was affected by the addition of verapamil to the apical side. Using a higher concentration of H 216/44 (5 mM) and addition of verapamil increased P_c of H 216/44 from $0.047 \pm 0.003 \times 10^{-6}$ to $0.104 \pm 0.016 \times 10^{-6}$ cm/s in the a−b direction and decreased P_c from $0.859 \pm 0.093 \times 10^{-6}$ to $0.265 \pm 0.052 \times 10^{-6}$ cm/s in the b−a direction. Thus the largest effect was seen on the b−a transport.
(54) Lundqvist, A.; Ocklind, G.; Haneskog, L.; Lundahl, P. Freeze−thaw-immobilization of liposomes in chromatographic gel beads: Evaluation by confocal microscopy and effects of freezing rate. In press.
(55) Brekkan, E.; Yang, Q.; Viel, G.; Lundahl, P. Immobilization of liposomes and proteoliposomes in gel beads. In *Methods in Biotechnology, Vol 1: Immobilization of Enzymes and Cells;* Bickerstaff, G. F., Ed.; Human Press Inc.: Totowa, NJ, 1997; pp 193−206.
(56) Artursson, P.; Ungell, A.-L.; Löfroth, J.-E. Selective paracellular permeability in two models of intestinal absorption: cultured monolayers of human intestinal epithelial cells and rat intestinal segments. *Pharm. Res.* **1993,** *10,* 1123−1129.
(57) Lee, B.; Richards, F. M. The interpretation of protein structures: estimation of static accessibility. *J. Mol. Biol.* **1971,** *55,* 379−400.

JM980313T